Immunomodulation of voltage-dependent K⁺ channels in macrophages: molecular and biophysical consequences

Núria Villalonga,[1] Miren David,[2] Joanna Bielanska,[1] Rubén Vicente,[1] Núria Comes,[1] Carmen Valenzuela,[2] and Antonio Felipe[1]

[1]Molecular Physiology Laboratory, Departament de Bioquímica i Biología Molecular, Institut de Biomedicina, Universitat de Barcelona, E-08028 Barcelona, Spain
[2]Instituto de Investigaciones Biomédicas "Alberto Sols," (CSIC-UAM), E-28029 Madrid, Spain

Voltage-dependent potassium (K_v) channels play a pivotal role in the modulation of macrophage physiology. Macrophages are professional antigen-presenting cells and produce inflammatory and immunoactive substances that modulate the immune response. Blockage of K_v channels by specific antagonists decreases macrophage cytokine production and inhibits proliferation. Numerous pharmacological agents exert their effects on specific target cells by modifying the activity of their plasma membrane ion channels. Investigation of the mechanisms involved in the regulation of potassium ion conduction is, therefore, essential to the understanding of potassium channel functions in the immune response to infection and inflammation. Here, we demonstrate that the biophysical properties of voltage-dependent K^+ currents are modified upon activation or immunosuppression in macrophages. This regulation is in accordance with changes in the molecular characteristics of the heterotetrameric $K_v1.3/K_v1.5$ channels, which generate the main K_v in macrophages. An increase in K^+ current amplitude in lipopolysaccharide-activated macrophages is characterized by a faster C-type inactivation, a greater percentage of cumulative inactivation, and a more effective margatoxin (MgTx) inhibition than control cells. These biophysical parameters are related to an increase in $K_v1.3$ subunits in the $K_v1.3/K_v1.5$ hybrid channel. In contrast, dexamethasone decreased the C-type inactivation, the cumulative inactivation, and the sensitivity to MgTx concomitantly with a decrease in $K_v1.3$ expression. Neither of these treatments apparently altered the expression of $K_v1.5$. Our results demonstrate that the immunomodulation of macrophages triggers molecular and biophysical consequences in $K_v1.3/K_v1.5$ hybrid channels by altering the subunit stoichiometry.

INTRODUCTION

Macrophages play an important role in the inflammatory responses triggered by hormones and cytokines. These cells, which also act as professional antigen-presenting cells, modify the cytokine milieu and the intensity of T cell signaling. Therefore, macrophages may tune the immune response toward inflammation or tolerance. The activation and proliferation of cells in the immune system are modulated by membrane transduction of extracellular signals. Some interactions occur via the regulation of transmembrane ion fluxes, and several studies suggest that some signaling occurs through ion movements in macrophages (Eder, 1998). Thus, macrophages change their membrane electrophysiological properties depending on their state of functional activation (Vicente et al.,

2003). Changes in membrane potential are among the earliest events occurring upon stimulation of macrophages, and ion channels underlie the Ca^{2+} signal involved in the leukocyte activation. In this context, potassium channels indirectly determine the driving force for Ca^{2+} entry (Cahalan and Chandy, 1997; Panyi et al., 2004).

Voltage-dependent potassium (K_v) channels have the crucial functions in excitable cells of determining the resting membrane potential and controlling action potentials (Hille, 2001). In addition, they are involved in the activation and proliferation of leukocytes (Cahalan and Chandy, 1997; Panyi et al., 2004). Accumulating evidence indicates that K_v channels play a pivotal role in the modulation of macrophage immunomodulatory responses. K_v channels are tightly regulated during proliferation and activation in macrophages, and their functional activity is important for cellular responses (Vicente et al., 2003, 2005, 2006, 2008;

Villalonga et al., 2007). Proliferation and activation trigger an induction of the outward K^+ current that is under transcriptional, translational, and posttranslational control (Vicente et al., 2003). Assigning specific K^+ channel clones to native currents is difficult because this complexity is further enhanced by the heteromultimeric assembly of different K_v subunits (Vicente et al., 2006). $K_v1.5$ coassociates with $K_v1.3$ to generate functional $K_v1.3/K_v1.5$ heterotetrameric channels in macrophages. In response to different physiological stimuli, changes in the oligomeric composition of functional K_v could have a crucial effect on intracellular signals, determining the specific macrophage response (Vicente et al., 2003, 2006, 2008; Villalonga et al., 2007).

Bacterial lipopolysaccharide (LPS) activates macrophages, leading to the secretion of bioactive molecules such as cytokines (e.g., TNF-α) and nitric oxide (NO) (Soler et al., 2001). However, there is tight regulation of signaling events to avoid an exaggerated response by macrophages during infection and injuries. These mechanisms include the release of glucocorticoids (GCs) by the adrenal gland. GCs, which exert their antiinflammatory action, in part, by influencing macrophages, inhibit the expression of inflammatory mediators, and thus are used in the treatment of many inflammatory diseases (Lloberas et al., 1998). GCs may trigger long-term changes in cell excitability by regulating K^+ channel gene expression. Thus, while macrophage activation induces $K_v1.3$, dexamethasone (DEX), a GC receptor agonist, inhibits $K_v1.3$ in T cells but differentially regulates $K_v1.5$ in several cells and tissues (Attardi et al., 1993; Takimoto et al., 1993; Takimoto and Levitan, 1994, 1996; Levitan et al., 1996; Lampert et al., 2003). Experimental evidence indicates that in macrophages, the major K_v is mainly a heterotetrameric $K_v1.3/K_v1.5$ channel (Vicente et al., 2006; Villalonga et al., 2007). Therefore, the analysis of macrophage hybrid channels under immunomodulation has physiological relevance. The aim of the present work was to investigate heteromeric $K_v1.3/K_v1.5$ channels in macrophages and to analyze the molecular and biophysical consequences upon activation and immunosuppression.

Here, we demonstrate that, in contrast to LPS, DEX inhibits $K_v1.3$. Neither LPS nor DEX apparently regulated $K_v1.5$ in macrophages, leading to different oligomeric $K_v1.3/K_v1.5$ channels. While LPS-induced activation increased, DEX diminished the $K_v1.3$ ratio in the complex. Protein and mRNA regulation correlated with the electrophysiological and pharmacological properties of the K^+ currents upon activation and immunosuppression. Our results demonstrate that different channel compositions change biophysical properties and could physiologically tune the membrane potential to achieve precise immune responses.

MATERIALS AND METHODS

Cell culture
Raw 264.7 macrophages were used. Cells were cultured in RPMI culture media containing 5% FBS supplemented with 2 mM L-glutamine and 10 U/ml penicillin and streptomycin. Cells were grown in 100-mm tissue culture dishes for sample collection and on noncoated glass coverslips for electrophysiology. In some experiments, Raw 264.7 cells were incubated with 100 ng/ml LPS and 1 µM DEX (Sigma-Aldrich) for 24 h.

RNA isolation, reverse transcription (RT)-PCR analysis, and real-time PCR
Total RNA from rat tissues (brain and heart), Jurkat T cells, L6E9 myoblasts, and Raw 264.7 macrophages were isolated using the Tripure reagent (Roche). All animal handling was approved by the ethics committee of the University of Barcelona in accordance with European Union regulations. RNA was treated with DNase I, and PCR controls were performed in the absence of RT. cDNA synthesis was performed using transcriptor RT (Roche) with a random hexanucleotide and oligo dT according to the manufacturer's instructions. Once cDNA was synthesized, the conditions were set for further PCR: 92°C for 30 s, 55°C for 1 min, and 72°C for 2 min. These settings were applied for 30 cycles. Primer sequences and accession numbers were: $K_v1.3$ (GenBank accession number M30441), F: 5'-CTCATCTCCATTGTCATCTTCTGA-3' and R: 5'-TTGAATTGGAAACAATCAC-3' (base pairs length: 718); $K_v1.5$ (GenBank accession number AF302768), F: 5'-GGATCACTC-CATCACCAG-3' and R: 5'-GGCTTCCTCCTCTTCCTTG-3' (base pairs length: 334). 10 µL from the final RT-PCR reactions was electrophoresed in a 1% agarose TBE gel (40 mM Tris, 20 mM acetic acid, and 1 mM EDTA, pH 8.0).

Real-time PCR was performed using a LightCycler machine (Roche) with LightCycler FastStart DNA Master[PLUS] SYBR Green I (Roche), according to the manufacturer's instructions. PCR primers were: $K_v1.5$, F: 5'-TCCGACGGCTGGACTCAATAA-3' and R: 5'-CAGATGGCCTTCTAGGCTGTG-3' (base pairs length: 133); $K_v1.3$, F: 5'-AGTATATGGTGATCGAAGAGG-3' and R: 5'-AGT-GAATATCTTCTTGATGTT-3' (base pairs length: 136). The reactions were performed under the following conditions: 95°C for 5 s, 55°C for 8 s, and 72°C for 9 s, preceded by 10 min at 95°C and followed by 10 min at 95°C. Melting curves were performed to verify the specificity of the product, and 18S (GenBank accession number X00686; F: 5'-CGCAGAATTCCCACTCCCGACCC-3' and R: 5'-CCCAAGCTCCAACTACGAGC-3'; base pairs length: 212) was included as an internal reference, as described previously. Results were analyzed with Light Cycler software 3.5 (Roche). For each primer set, a standard curve was made and the slope factor calculated. Values were normalized to the corresponding 18S. The corresponding real-time PCR efficiency (E) of one cycle in the exponential phase was calculated according to the equation: $E = 10^{(-1/slope)}$. The normalized $K_v1.5/K_v1.3$ ratio was calculated as follows: Ratio = $(1+E)^{\Delta Ct(Kv1.5)}/(1+E)^{\Delta Ct(Kv1.3)}$, where Ct signifies the threshold cycle.

Crude membrane preparations and Western blot
Cells were washed twice in cold PBS and lysed on ice with lysis solution (1% Triton X-100, 10% glycerol, 50 mM HEPES, pH 7.5, and 150 mM NaCl) supplemented with 1 µg/ml aprotinin, 1 µg/ml leupeptin, 1 µg/ml pepstatin, and 1 ml phenylmethylsulfonyl fluoride as protease inhibitors. To obtain enriched membrane preparations, homogenates were centrifuged at 3,000 g for 10 min, and the supernatant was further centrifuged at ~150,000 g for 90 min. The pellet was resuspended in 30 mM HEPES, pH 7.4, and protein content was determined by the Bio-Rad Protein Assay (Bio-Rad Laboratories). Samples were aliquoted and stored at −80°C.

Crude membrane protein samples (50 µg) were boiled in Laemmli SDS loading buffer and separated on 10% SDS-PAGE. Next, they were transferred to nitrocellulose membranes (Immobilon-P; Millipore) and blocked in 5% dry milk–supplemented 0.2% Tween 20 PBS before immunoreaction. Filters were immunoblotted with antibodies against $K_v1.3$ (1/200; Alomone Labs), $K_v1.5$ (1/500; Alomone Labs), and inducible NO synthase (iNOS; 1/500; Santa Cruz Biotechnology, Inc.). As a loading and transfer control, a monoclonal anti–β actin antibody (1/5,000; Sigma-Aldrich) was used. The specificity of $K_v1.3$ and $K_v1.5$ commercial antibodies was tested with control antigen peptides provided by the manufacturer. Densitometric analysis of the filters was performed by Phoretix software (Nonlinear Dynamics). Results are presented as the mean ± SEM of each experimental group.

Electron microscopy

Macrophages were fixed in 4% paraformaldehyde (PFA)/0.2% glutaraldehyde (GA) in PBS for 30 min at room temperature, and then left in 2% PFA/0.1% GA in PBS overnight at 4°C. Fixation was stopped by washing with 20 mM glycine in PBS. Cells were scraped and collected in tubes (Eppendorf) with 12% gelatin. After solidifying on ice, gelatin blocks were infiltrated in 2.3 M sucrose in PBS overnight at 4°C. Blocks were frozen in liquid nitrogen. Ultrathin cryosections were obtained using Leica ULTRACUT EM FCS at −118°C and subjected to immunogold labeling. Cryosections were incubated at room temperature on drops of 2% gelatin in phosphate buffer for 20 min at 37°C, followed by 50 mM glycine in PBS for 15 min and 5% normal goat serum (NGS) in PBS for 10 min. Then they were incubated with anti-$K_v1.5$ and anti-$K_v1.3$ polyclonal antibodies in 5% NGS in PBS for 30 min. After three washes with drops of 5% NGS in PBS for 20 min, sections were incubated for 60 min using immunoglobulin G anti–rabbit coupled to 10- or 15-nm diameter colloidal gold particles (Aurion) using a 1:60 dilution in 5% NGS in PBS. This was followed by three washes with drops of PBS for 10 min and two washes with distilled water. As a control for nonspecific binding of the colloidal gold–conjugated antibody, the primary polyclonal antibody was omitted. Finally, the cryosections were contrasted and embedded in a mixture of methylcellulose and uranyl acetate. For the double immunogold, immunolabeling with one of the primary antibodies was done. We used the secondary antibody conjugated with the small gold (10 nm) in the first immunolabeling procedure. Then, the anti–immunoglobulin G binding sites were inactivated using 3% PFA/2% GA in PBS for 2 h. After inactivation, the immunolabeling with the other primary antibody was done using the secondary antibody conjugated to 15-nm gold particles. Primary antibody dilutions were 1:50 in both cases. Samples were viewed with an electron microscope (1010; JEOL).

Electrophysiological recordings

Whole cell currents were measured using the patch clamp technique with an amplifier (Axopatch 1C; Axon Instruments) and stored on a personal computer (TD Systems) with an analogue-to-digital converter (DigiData 1322A; Axon Instruments). pClamp version 9 software (Axon Instruments) was used for data acquisition and analysis. Currents were recorded at room temperature (21–23°C) at a stimulation frequency of 0.1 Hz and sampled at 4 kHz after anti-alias filtering at 2 kHz. Patch electrodes of 2–4 MΩ were fabricated in a puller (P-87; Sutter Instrument Co.) from borosilicate glass capillary tubes (GD-1; Narishige). GigaΩ seal formation was achieved by suction (2–5 GΩ; $n = 12$). After seal formation, cells were lifted from the bath and the membrane patch was ruptured with a brief additional suction. The capacitive transients elicited by symmetrical 10-mV steps from −80 mV were recorded at 50 kHz and filtered at 10 kHz for subsequent calculations of capacitive surface area, access resistance, and input impedance.

Thereafter, capacitance and series resistance compensation were optimized and, usually, 80% compensation of the effective access resistance was obtained. Electrodes were filled with an intracellular pipette solution containing (in mM): 80 K-aspartate, 50 KCl, 3 phosphocreatine, 10 KH_2PO_4, 3 MgATP, 10 HEPES-K, and 5 EGTA-K, and was adjusted to pH 7.25 with KOH. The bath solution contained (in mM): 130 NaCl, 4 KCl, 1.8 $CaCl_2$, 1 $MgCl_2$, 10 HEPES-Na, and 10 glucose, and was adjusted to pH 7.40 with NaOH. Uncompensated series resistances were 4–8 MΩ, as currents evoked were <1 nA; voltage errors from uncompensated series resistance were <2 mV.

Inactivation was fit to an exponential process, using an equation of the form:

$$y = A_1 \exp(-t/\tau_1) + C$$

where τ is the system time constant, A is the amplitude, and C is the baseline value. To analyze the cumulative inactivation, currents were elicited by a train of eight depolarizing voltage steps of 200 ms to + 60 mV once every 400 ms. The voltage dependence of activation curves were fitted with a Boltzmann equation:

$$y = 1/\left[1 + \exp\left(-\left(V - V_h\right)/k\right)\right],$$

in which k represents the slope factor, V the membrane potential, and V_h the voltage at which 50% of the channels are open (Franqueza et al., 1998; González et al., 2001).

The number of channels per cell and their surface density were calculated from the conductance of $K_v1.3$ (13 pS) and $K_v1.5$ (8 pS) following the $K_v1.3/K_v1.5$ ratio obtained from real-time PCR results following the equation:

$$G = I_{max}/\left(V - V_K\right),$$

where G represents the total conductance, I_{max} is the peak amplitude, V is the voltage applied, and V_K is the K^+ equilibrium potential.

To characterize the K^+ current pharmacologically, 750 pM margatoxin (MgTx; Alomone Labs) was added to the external solution (Vicente et al., 2003, 2006). Toxin was reconstituted at 10 µM in Tris buffer (0.1% BSA, 100 mM NaCl, and 10 mM Tris, pH 7.5). Solutions were perfused by using a gravity-flow perfusion setup. The inhibition by MgTx was defined by the remaining current fraction in the presence and absence of the toxin. All recordings were performed at room temperature (20–23°C).

Lentivirus infection

To knock down $K_v1.3$ in Raw macrophages, $K_v1.3$ shRNA (mouse) lentiviral (LTV) particles were used (Santa Cruz Biotechnology, Inc.). Cells were cultured in 12-well dishes to get ∼50% confluence and infected with 5,000 infectious units in the presence of 2 µg/ml polybrene (Sigma-Aldrich). 24 h after infection, the medium was replaced by regular culture medium supplemented with 10 µg/ml puromycin (Sigma-Aldrich) for clone selection. Selected clones were maintained with 2 µg/ml puromycin. Specific silenced expression of $K_v1.3$, but not $K_v1.5$, was confirmed by Western blot. Control shRNA LTV particles containing a scrambled sequence were also used (not depicted).

Statistics

Values are expressed as the mean ± SEM. The significance of differences was established by Student's t test or Pearson product-moment correlation coefficient with a two-tailed p-value (PRISM 4.0; GraphPad Software, Inc.) when indicated. The curve-fitting procedure used a nonlinear least-squares (Gauss-Newton) algorithm; results were displayed in linear format. Goodness of fit was

judged by the χ^2 criterion and by inspection for systematic non-random trends in the difference plot. A value of $P < 0.05$ was considered significant.

RESULTS

$K_v1.3$ and $K_v1.5$ generate K_v currents in Raw 264.7 macrophages

K_v currents were evoked in Raw cells by applying depolarizing pulses from a holding potential of -80 mV to different depolarizing voltages from -80 to $+60$ mV in 10-mV steps (Fig. 1 A). Fig. 1 B plots normalized conductance against test potential. The threshold for activation was about -20 mV. V_h and k slope were 11.1 ± 2.2 and 12.3 ± 2.5 mV, respectively. Previous work indicates that macrophages exhibit K_v currents mainly generated by $K_v1.3$ and $K_v1.5$ channels (Vicente et al., 2003, 2005, 2006, 2008; Villalonga et al., 2007). Therefore, we analyzed the presence of these channels in Raw macrophages. To analyze the K^+ channel mRNA expression, we performed RT-PCR analysis. Mouse brain and heart RNAs were used as positive controls for $K_v1.3$ and $K_v1.5$, respectively. Fig. 1 C demonstrates that $K_v1.3$ and $K_v1.5$ mRNA were detected in Raw macrophages in the presence (+RT), but not in the absence, of the retrotranscriptase ($-RT$). In addition, a specific $K_v1.3$ and $K_v1.5$ signal was obtained by Western blot (Fig. 1 D). As

expected, $K_v1.3$ protein was detected in macrophages and Jurkat T cells, whereas Raw cells shared $K_v1.5$ expression with L6E9 skeletal muscle myoblasts (Villalonga et al., 2008). We have recently shown that although $K_v1.3$ may form homotetrameric structures, and may be located at the membrane surface, $K_v1.5$ mostly coassociates with $K_v1.3$ to form heterotetrameric channels in macrophages (Vicente et al., 2006; Villalonga et al., 2007). In addition, the presence of $K_v1.5$ impairs the membrane surface location of the complex (Martínez-Mármol et al., 2008; Vicente et al., 2008). Electron microscopic immunocytochemical detection studies with specific antibodies showed that although $K_v1.3$ was detected at the membrane surface, many heteromeric structures containing $K_v1.5$ were located intracellularly (Fig. 1 E). Collectively, these data indicate that Raw 264.7 macrophages have outward delayed rectifier K^+ currents that are mainly conducted by $K_v1.3$ and $K_v1.5$ channels.

Immunomodulation of macrophages triggers differential biophysical and pharmacological consequences

Once K_v currents were characterized and the molecular basis of the responsible channels was identified, we next analyzed their biophysical characteristics upon activation or immunosuppression in macrophages (Fig. 2). Raw cells were either activated with LPS or cultured in
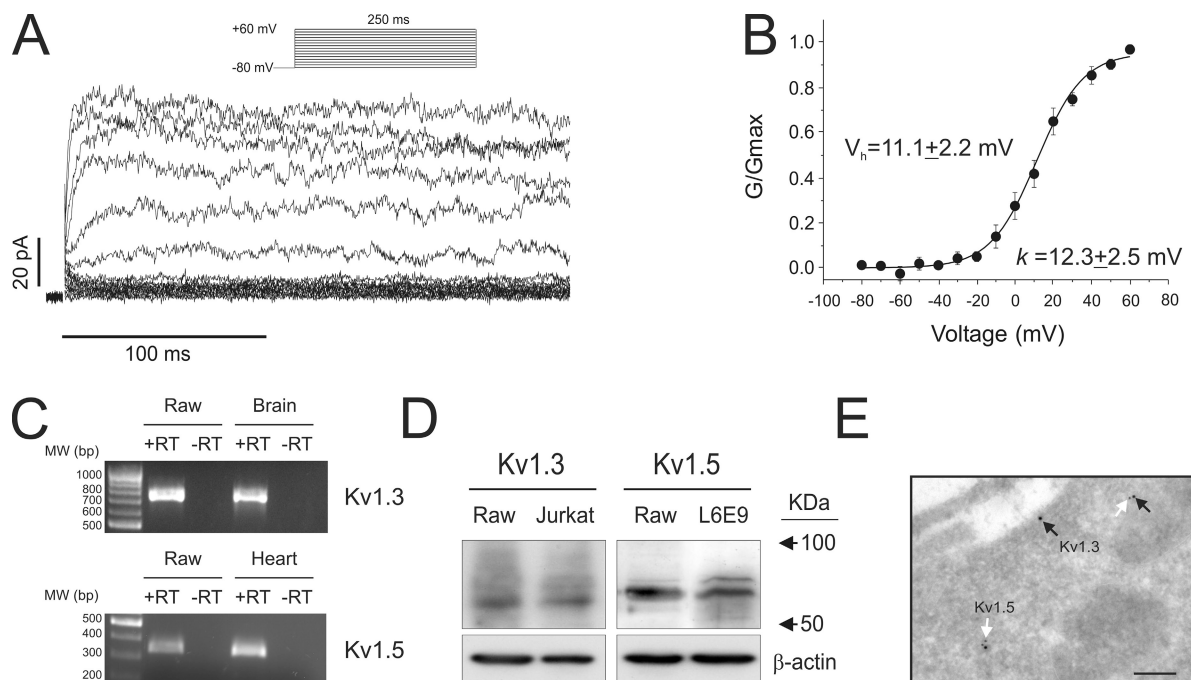

Figure 1. Macrophages express $K_v1.3$ and $K_v1.5$. Cells were held at -80 mV, and pulse potentials were applied as indicated. (A) Representative traces of delayed rectifier K^+ currents. (B) Steady-state activation curve of the outward current. Conductance was plotted against test potentials. (C) mRNA expression of $K_v1.3$ and $K_v1.5$ in Raw 264.7 cells. Mouse brain and heart RNA were used as positive controls for $K_v1.3$ and $K_v1.5$, respectively. PCR reactions were performed in the presence (+) or absence ($-$) of the retrotranscriptase reaction. (D) $K_v1.3$ and $K_v1.5$ protein expression in Raw macrophages. Jurkat T lymphocytes and L6E9 skeletal muscle myoblasts were used as positive controls for $K_v1.3$ and $K_v1.5$, respectively. (E) Immunocytochemical electron microscopic detection of $K_v1.3$ and $K_v1.5$ proteins. Arrows show specific channel protein localization. Black arrow, $K_v1.3$; white arrow, $K_v1.5$; bar, 0.20 μm.

the presence of DEX. Fig. 2 A shows representative traces from a single depolarizing 250-ms pulse potential from -80 to $+60$ mV. Unlike DEX, LPS slightly increased the peak current amplitude. However, the inactivation time course was clearly affected by both treatments. While LPS accelerated, DEX slowed it. The effects of LPS and DEX on Raw cells were analyzed as the changes in current density observed at different test potentials during the application of 250-ms depolarizing pulses from -80 to $+60$ mV in 10-mV steps. The current density versus voltage relationships are depicted in Fig. 2 B. Once the channels opened (above -20 mV), LPS, but not DEX, increased currents at all depolarizing voltages applied (from -20 to $+60$ mV). While LPS increased peak currents (at $+60$ mV) up to twofold, DEX slightly decreased the current amplitude (Fig. 2 C). This apparent discrepancy between current amplitudes and current densities was related to the size of the cell. Raw cells incubated with LPS were $\sim 40\%$ smaller than control cells (Fig. 2 D). On the other hand, apparently DEX did not modify the cell size.

The number and density of the channels increased during LPS-induced activation (Fig. 2, E and F, respectively).

While at $+60$ mV, resting cells expressed ~ 60 channels/cell with a density of ~ 0.018 channel/μm^2, and activated cells showed ~ 82 channels/cell and ~ 0.04 channel/μm^2 ($P < 0.05$ and $P < 0.001$ vs. control for number and density, respectively). On the other hand, DEX did not modify the number or the density of the channels.

Different $K_v 1.3 / K_v 1.5$ hetero-oliogomeric structures lead to distinct pharmacological properties of the channel (Vicente et al., 2006). Although $K_v 1.3$ and $K_v 1.3 / K_v 1.5$ heteromeric channels are sensitive to MgTx, a highly specific $K_v 1.3$ blocker, $K_v 1.5$ homotetrameric structures are resistant (Vicente et al., 2006). As described previously (Villalonga et al., 2007), pharmacological analysis of the K_v currents in the presence of MgTx demonstrated that K^+ currents were fully sensitive to MgTx in Raw macrophages (not depicted). When K^+ currents were analyzed in the presence of 750 pM MgTx, a concentration close to the IC_{50} of the toxin (Villalonga et al., 2007), K^+ currents were inhibited (Fig. 3 A). The efficiency of MgTx in LPS-treated macrophages was noticeable, as the majority of LPS-dependent, induced K^+ current was blocked (Fig. 3 A). The percentage of inhibition of the peak current density at $+60$ mV in the presence of MgTx (Fig. 3 B) indicated that
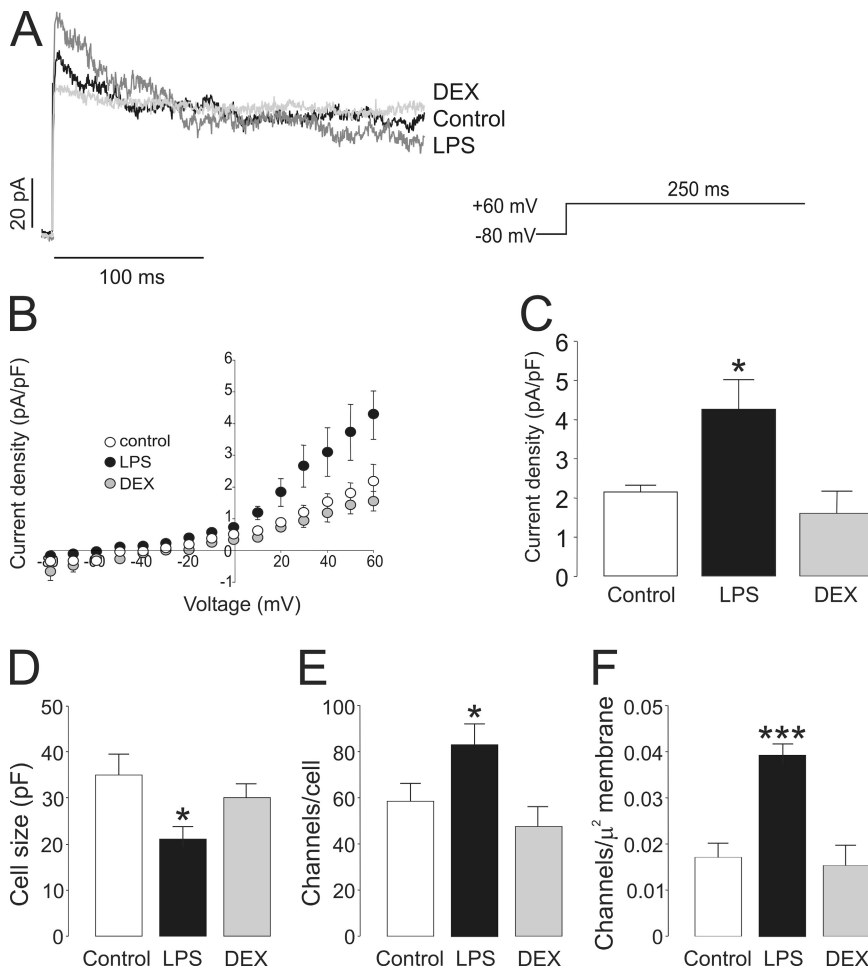

Figure 2. Voltage-dependent K^+ currents in Raw 264.7 macrophages. (A) Representative traces of delayed rectifier K^+ currents in control, LPS-, and DEX-treated cells. Macrophages were treated with 100 ng/ml LPS and 1 μM DEX for 24 h. Cells were held at -80 mV, and currents were elicited by a depolarizing pulse to $+60$ mV (250-ms duration). Black trace, control; dark gray trace, LPS; light gray trace, DEX. (B) Current density (pA/pF) versus voltage relationship of K^+ currents. Current density was calculated as a function of peak amplitude and the cell capacitance of each recorded cell. (C) Peak current density at $+60$ mV. (D) Cell capacitance (pF) from the same cell population from B. (E) Channel density was calculated from the conductance of $K_v 1.3$ (13 pS) and $K_v 1.5$ (8 pS) following the real-time PCR results in Fig. 4 and the $K_v 1.3 / K_v 1.5$ ratio shown in Fig. 8. (F) The results in E as a function of the plasma cell membrane surface. White (bar or circle), control; black (bar or circle), LPS; gray (bar or circle), DEX. *, $P < 0.05$; ***, $P < 0.001$ versus control; $n > 10$ cells per group (Student's t test).
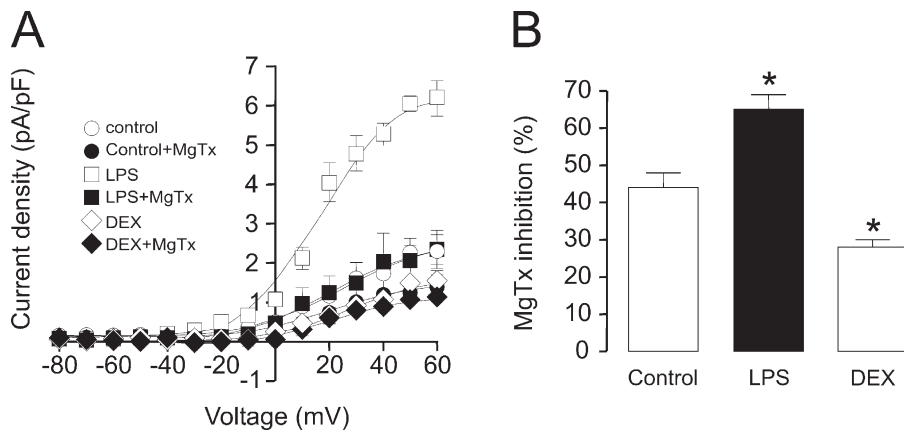
Figure 3. MgTx inhibits K⁺ currents in macrophages. Cells were held at −80 mV, and pulse potentials were applied as indicated in Fig. 1 in the presence or absence of 750 pM MgTx. (A) Current density (pA/pF) versus voltage relationship of K⁺ currents. Current density was calculated as a function of the peak amplitude and the capacitance for each recorded cell in the presence (black symbols) and absence (white symbols) of MgTx. (B) Percentage of MgTx inhibition at the peak current density (+60 mV). White bar, control; black bar, LPS; gray bar, DEX. *, P < 0.05 versus control; n = 4–6 cells per group (Student's t test).

while in control cells the current was blocked 44 ± 3%, this inhibition was 65 ± 4 and 28 ± 2% in the presence of LPS and DEX, respectively (n = 4–6; P < 0.05 vs. control). These results further confirm that although $K_v1.3$ could form homomeric channels in macrophages, $K_v1.5$ mostly coassociates with $K_v1.3$ to generate multiple heteromeric structures with distinct pharmacological properties.

Differential expression of $K_v1.3$ and $K_v1.5$ upon activation and immunosuppression

Fig. 4 A illustrates the $K_v1.3$ and $K_v1.5$ gene expression after the addition of LPS and DEX. Although $K_v1.3$ is differentially regulated by LPS and DEX, $K_v1.5$ remained almost unchanged. However, although the expression of $K_v1.3$ increased up to 2.5-fold in LPS-treated macrophages, its expression decreased by 50% in the presence of DEX. Similar changes were obtained for the $K_v1.3$ and $K_v1.5$ protein abundance in macrophages incubated for 24 h in the presence of LPS and DEX (Fig. 4 B). No differences were observed with $K_v1.5$ throughout the study. The expression of the iNOS was used as a marker of macrophage activation (Soler et al., 2001). As expected, iNOS was induced in the presence of LPS, but not DEX. Fig. 4 (C and D) represents the quantification of at least three independent blots. Collectively, these data indicate that LPS-induced activation led to long-term increases in current densities of outward K⁺ currents in accordance with an induction in $K_v1.3$ mRNA and protein expression. On the contrary, DEX, which slightly decreased current densities, decreased $K_v1.3$ expression. Because neither LPS nor DEX incubation produced K⁺ currents resistant to MgTx (not depicted), our results are consistent with an increased or decreased number of $K_v1.3$ subunits, either as homomeric $K_v1.3$ or hybrid $K_v1.3/K_v1.5$ channels upon activation or immunosuppression.

Inactivation properties are differentially regulated during immunomodulation

As demonstrated (Fig. 2 A), K_v currents recorded from Raw cells inactivate with a different time course in the
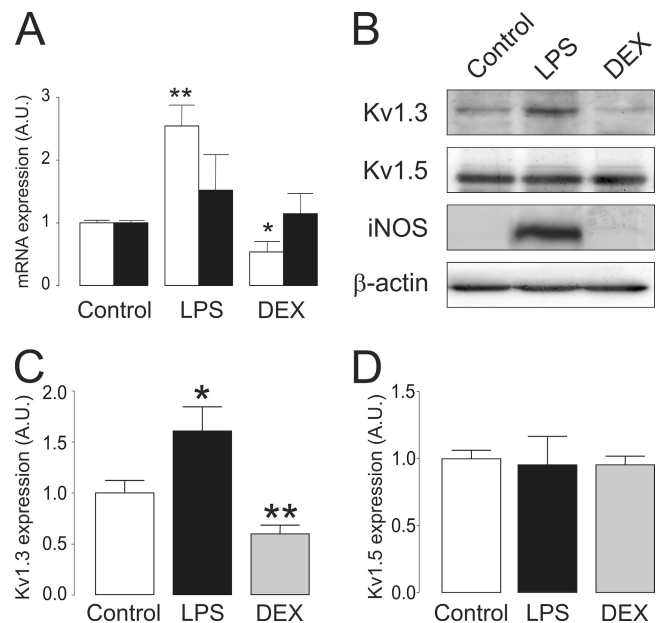

Figure 4. Activation and immunosuppression differentially regulates $K_v1.3$ and $K_v1.5$ in macrophages. Control cells were incubated for 24 h in the presence of LPS and DEX. Samples were collected after the addition of agents, and $K_v1.3$ and $K_v1.5$ expression was analyzed. (A) $K_v1.3$ (white bar) and $K_v1.5$ (black bar) relative mRNA expression by real-time PCR. Values are the mean ± SEM (n = 4). Significant differences were only found with $K_v1.3$ (*, P < 0.05; **, P < 0.01 vs. control; Student's t test). Using standard curves, fold variation in arbitrary units (A.U.) was normalized to 18S relative quantity (RQ) as follows: ($K_v1.5$ or $K_v1.3$ RQ (LPS or DEX)/18S RQ (LPS or DEX))/($K_v1.5$ or $K_v1.3$ RQ (control)/18S RQ (control)). (B) $K_v1.3$, $K_v1.5$, and iNOS protein expression in macrophages. Representative blots are shown. (C and D) $K_v1.3$ (C) and $K_v1.5$ (D) quantification of data in B. Values were normalized to β actin. In all cases, arbitrary units are standardized to the control value in the absence of treatment. White bars, control; black bars, LPS; gray bars, DEX. Values are the mean ± SEM of at least three independent experiments. *, P < 0.05; **, P < 0.01 versus control (Student's t test).

absence or presence of LPS or DEX. Inactivation parameters are useful to evaluate possible differences in the tetrameric K⁺ channel phenotype. $K_v1.3$ is well
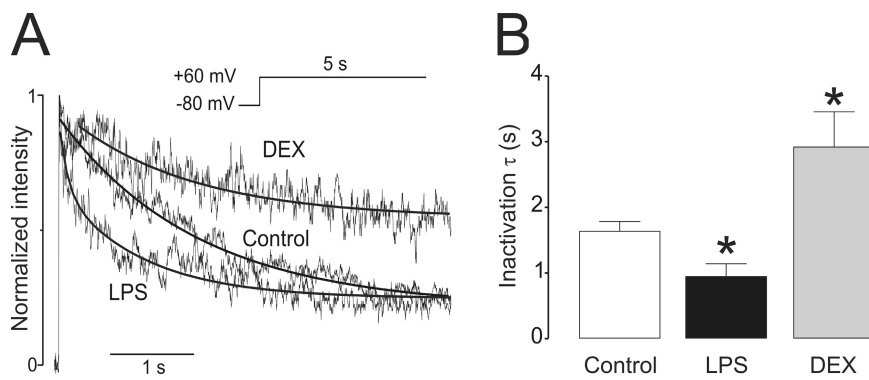
Figure 5. Biophysical properties of the C-type inactivation of K$^+$ currents in Raw macrophages. (A) Representative traces of C-type inactivation. Cells were held at -80 mV, and pulse potentials were applied from -80 to $+60$ mV for 5 s. For comparison, the intensity in each group has been normalized. (B) Time constant of inactivation (τ). Values are the mean $\pm$ SEM of at least 10 independent cells. *, P < 0.05 versus control (Student's *t* test).

characterized by its C-type inactivation, which is absent in K$_v$1.5 (Po et al., 1992; Gutman et al., 2005). Because C-type inactivation involves the cooperative interaction of all four subunits, this parameter could be used to determine heterotetramers (Panyi et al., 1995). Fig. 5 shows the time course of K$^+$ current inactivation after applying a depolarizing pulse from -80 to $+60$ mV for 5 s (Fig. 5 A). Although K$^+$ currents inactivated with a time constant of inactivation of $1,630 \pm 40$ ms ($n = 5$) in control macrophages, in LPS-treated cells, it was 885 ± 35 ms ($n = 6$; P < 0.05 vs. control). However, this process

became much slower in Raw cells treated with DEX ($2,940 \pm 70$ ms; $n = 5$; P < 0.05 vs. control) (Fig. 5 B). Our results further support the notion that K$_v$ currents generated upon depolarization in macrophages are generated by K$_v$ channels with different subunit stoichiometry upon activation or immunosuppression.

Cumulative inactivation of certain K$^+$ channels is characterized by an inactivation that accumulates during repetitive depolarizing pulses because recovery during the interpulse interval is incomplete (Grissmer et al., 1994). Fig. 6 (A–C) depicts representative traces of K$^+$
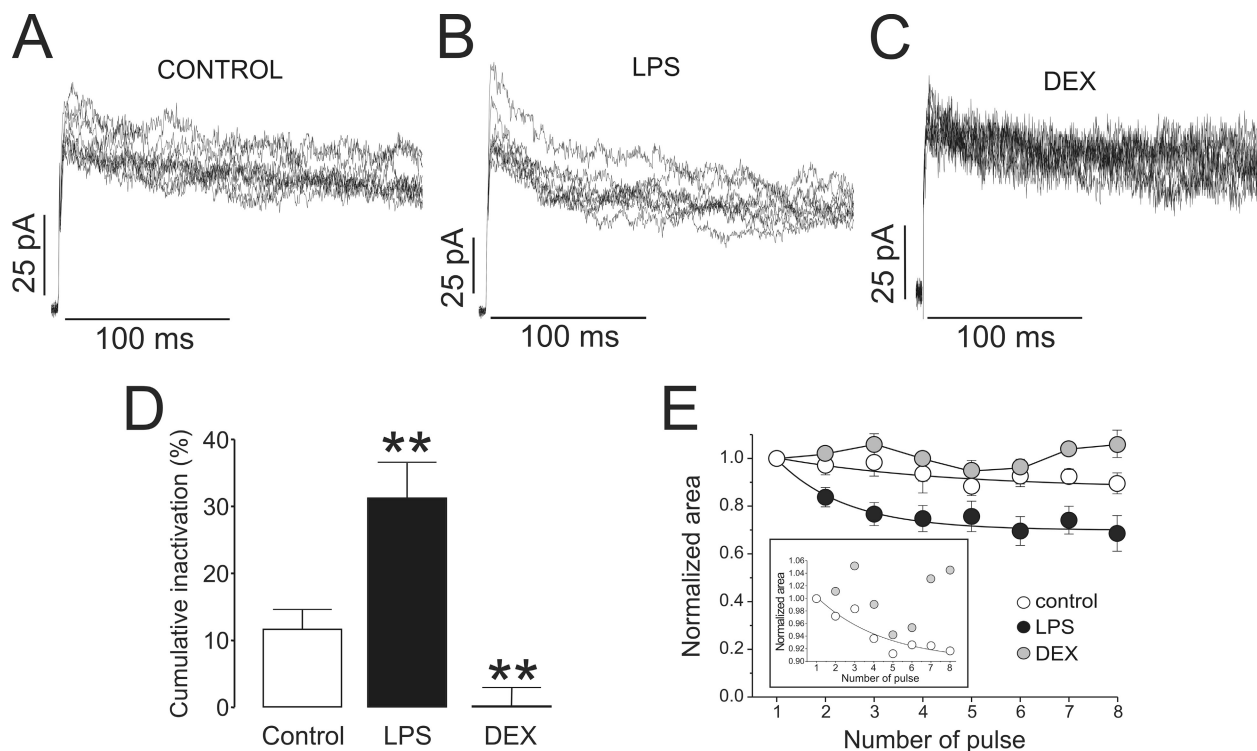

Figure 6. Biophysical properties of the cumulative inactivation of K$^+$ currents in Raw macrophages. (A–C) Representative traces showing cumulative inactivation of K$^+$ currents. Cells were held at -80 mV, and currents were elicited by a train of eight depolarizing voltage steps (200-ms duration) to $+60$ mV once every 400 ms. (A) Control. (B) LPS. (C) DEX. (D) Percentage of cumulative inactivation at the peak current. The percentage was calculated as a result of the difference between the peak current at the first pulse and the remaining current at the last. (E) Plot of normalized current area versus pulse. The current amplitude became progressively smaller from the first trace to the last in control and LPS, but not in DEX-treated macrophages. Inset represents K$^+$ current area decay from control and DEX-treated macrophages for magnification. Values are the mean $\pm$ SEM of at least 10 independent cells. **, P < 0.01 versus control (Student's *t* test).

currents in macrophages in the presence and absence of LPS or DEX during the application of a train of repetitive pulses, each of 200 ms at a frequency of 4 Hz. The standardized peak current amplitude rapidly diminished in control Raw cells (Fig. 6 A). In LPS-activated macrophages, the accumulation of inactivation increased (Fig. 6 B). However, this was much less apparent in Raw cells treated with DEX (Fig. 6 C). Although the cumulative inactivation was $12 \pm 3\%$ ($n = 7$) in control cells, in LPS-induced cells, activation rose to $31 \pm 6\%$ ($n = 7$; P < 0.01 vs. control) (Fig. 6 D). In contrast, incubation with DEX led to a marked decrease, and cumulative inactivation was almost absent (0.5 ± 3; $n = 7$; P < 0.01 vs. control). The normalized area of the K$^+$ currents demonstrated that, contrary to DEX, cumulative inactivation was noticeable in control and LPS-activated macrophages from the first pulse (Fig. 6 E). Once again, these results indicate that K$_v$1.5 associates with K$_v$1.3, forming different heteromeric structures, and this stoichiometry may be changed by different stimuli.

K$_v$1.3 gene silencing in Raw 264.7 macrophages counteracts LPS-dependent biophysical changes

LPS and DEX regulated K$_v$1.3 expression in agreement with changes in electrophysiological properties, which suggest changes of K$_v$1.3 subunits either as K$_v$1.3 homotetrameric or K$_v$1.3/K$_v$1.5 heterotetrameric channels. Therefore, we next analyzed whether K$_v$1.3 gene silencing impairs LPS and DEX modulation. LTV shRNA K$_v$1.3 infection in macrophages led to an ∼65% decrease in K$_v$1.3 protein expression (Fig. 7 A). Although macroscopic outward K$^+$ currents were similar between control (Raw) and LTV-infected cells (Raw-LTV), K$^+$ currents in LTV cells were slightly lower and inactivate less than control (Fig. 7 B). Fig. 7 C demonstrates that neither LPS nor DEX modulated the current density in LTV cells. However, LPS still triggered changes in the cell size (Fig. 7 D). Unlike in Raw macrophages, 5-s pulses did not inactivate currents in Raw-LTV cells (Fig. 7 E). In addition, LPS and DEX did not significant modify the time constant for inactivation in LTV cells.
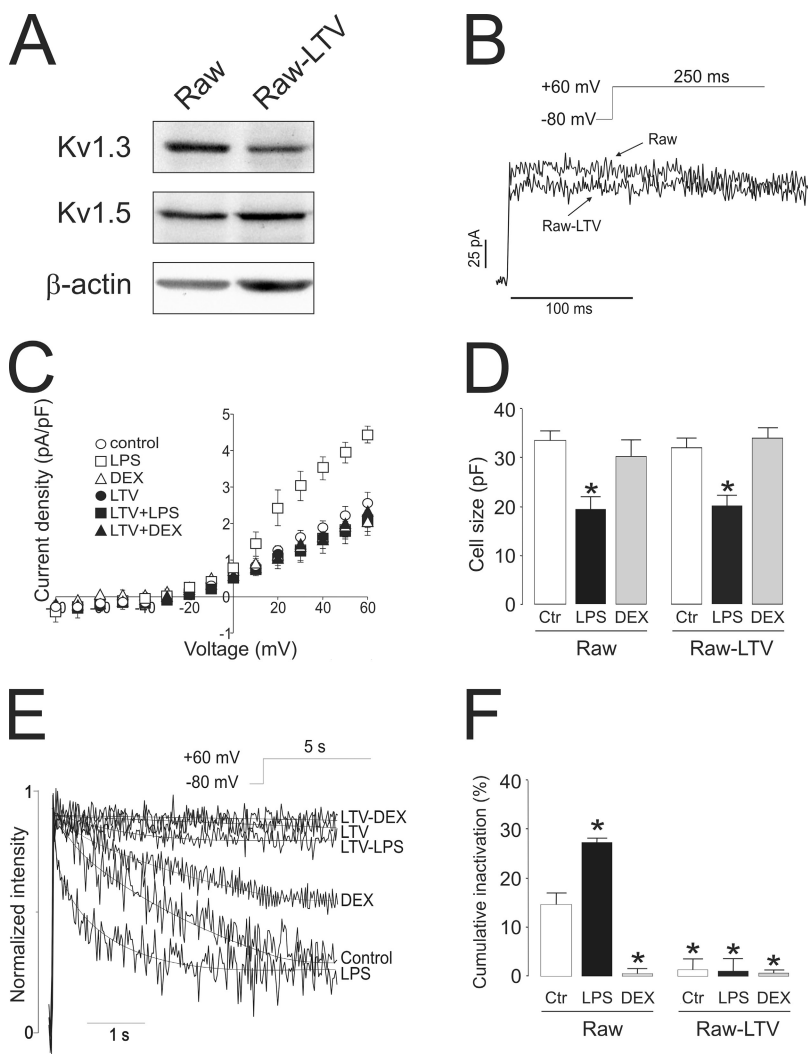

Figure 7. K$_v$1.3 gene silencing abolishes LPS- and DEX-dependent biophysical changes in macrophages. LTV shRNA (mouse) K$_v$1.3 was used to silence the K$_v$1.3 gene in Raw 264.7 macrophages. (A) A representative Western blot. Note that although K$_v$1.3 expression is lower in LTV, relative K$_v$1.5 abundance was similar in both groups. Raw, control macrophages; Raw-LTV, LTV-silenced K$_v$1.3 macrophages. (B) Representative traces of K$^+$ currents in macrophages. Cells were held at -80 mV, and currents were elicited by a depolarizing pulse to $+60$ mV (250-ms duration). (C) Current density (pA/pF) versus voltage relationship of K$^+$ currents. Current density was calculated as a function of peak amplitude and the capacitance of each recorded cell in the presence or absence of LPS and DEX. (D) Cell capacitance (pF) from the same cell population from B. (E) Representative traces of C-type inactivation. Cells were held at -80 mV, and pulse potentials were applied from -80 to $+60$ mV for 5 s. For comparison, the intensity in each group has been normalized. (F) Percentage of cumulative inactivation at the peak current. Cells were held at -80 mV, and currents were elicited by a train of eight depolarizing voltage steps (200-ms duration) to $+60$ mV once every 400 ms. The percentage was calculated as a result of the difference between the peak current at the first pulse and the remaining current at the last. (D and F) Raw, no infected Raw macrophages; Raw-LTV, lentivirus-infected Raw cells; white bars, control (no treatment); black bars, LPS; gray bars, DEX. Values are the mean $\pm$ SEM of six to eight independent cells. *, P < 0.001 versus control (Student's t test).

Cumulative inactivation was also affected in LTV cells (Fig. 7 F). Although LPS triggered an increase in Raw macrophages, DEX, LTV, and LTV-treated cells showed no inactivation. These results show that (a) K^+ currents in LTV cells did not recapitulate $K_v1.3$ characteristics, and (b) LPS and DEX incubation did not alter the electrophysiological phenotype.

Our results suggest that LPS and DEX regulated $K_v1.3$, leading to pharmacologically distinct channels. MgTx differentially inhibited K^+ currents upon activation and immunosuppression in Raw macrophages (Fig. 3). Therefore, we analyzed K_v currents in Raw-LTV cells in the presence of 750 pM MgTx. Unlike Raw control cells, K_v currents in Raw-LTV cells were highly resistant to the toxin. Thus, peak current densities (+60 mV) were 2.22 ± 0.02 versus 2.19 ± 0.12 pA/pF (control), 2.31 ± 0.02 versus 2.25 ± 0.03 pA/pF (LPS), and 2.33 ± 0.04 versus 2.28 ± 0.33 pA/pF (DEX) in the absence or presence of MgTx, respectively ($n = 4$–6).

DISCUSSION

As regulation of macrophage function involves ion channels, this study was performed to elucidate the influence of proinflammatory and antiinflammatory agents on macrophage K_v channel activity. Here, we describe, for the first time, that $K_v1.3/K_v1.5$ heteromeric channel expression and their biophysical and pharmacological properties change differentially upon activation and immunosuppression. Our results have physiological relevance indicating that K_v heteromeric expression is important as an early regulatory step, and that fine-tuning modulation of their expression is crucial to the specific membrane signaling that triggers the appropriate immune response. Activated macrophages secrete proinflammatory substances like cytokines (e.g., TNF-α) or NO with potential cellular toxicity (Xaus et al., 2001). This release activity is triggered by LPS (Soler et al., 2001). In previous work, we showed that LPS and TNF-α induce $K_v1.3$ in macrophages (Vicente et al., 2003, 2005, 2006; Villalonga et al., 2007). Those experiments were designed to characterize the regulation of individual channels. However, accumulating evidence indicates that $K_v1.3$ and $K_v1.5$ associate in mononuclear phagocytes to generate distinct hybrid channels (Villalonga et al., 2007; Martínez-Mármol et al., 2008; Vicente et al., 2008). In the present work, we address this issue, characterizing the effects of LPS on the $K_v1.3/K_v1.5$ heterotetrameric channel and analyzing biophysical and pharmacological consequences. Unlike $K_v1.5$, $K_v1.3$ was induced; therefore, heteromeric channels contain more $K_v1.3$ units in LPS-activated macrophages than in control ones. Because C-type and cumulative inactivation, which are $K_v1.3$ hallmarks, need the cooperative interaction of the four subunits (Panyi et al., 1995), the altered subunit stoichiometry was in accordance

with these biophysical changes. The presence of $K_v1.3$ at the membrane surface assures the specific activation, and the presence of $K_v1.5$ in the hybrid channel shifts the activation curve toward depolarizing potentials (Vicente et al., 2006). Indeed, a +25-mV change modifies interleukin 2 production, thus reducing the activation and the antibody production by lymphocytes (Freedman et al., 1992). In addition, as we have suggested previously and further confirmed here, $K_v1.3/K_v1.5$ heteromers tend to be more intracellular, fine-tuning the response (Vicente et al., 2008). Thus, $K_v1.5$ impairs the location of $K_v1.3$ in lipid raft microdomains, but this is partially reversed by incubation with LPS (Martínez-Mármol et al., 2008; Vicente et al., 2008). In fact, lipid rafts play a role in LPS-induced signaling in macrophages (Olsson and Sundler, 2006).

$K_v1.3$ is crucial to the immune response. However, the role of $K_v1.5$ in the myeloid lineage is under debate. Pyo et al. (1997) demonstrated that outward K^+ channels induced by LPS are immunologically related to $K_v1.5$. Furthermore, although some studies support the unique expression of $K_v1.3$ without an apparent function, others claim a pivotal role for $K_v1.5$ (Mackenzie et al., 2003; Park et al., 2006). However, most of the literature describes $K_v1.3$ and $K_v1.5$ in the myeloid lineage, and an association of the two proteins has been demonstrated (Kotecha and Schlichter, 1999; Vicente et al., 2003, 2005, 2006, 2008; Fordyce et al., 2005; Judge et al., 2006; Mullen et al., 2006; Pannasch et al., 2006; Villalonga et al., 2007). Indeed, microglia activation by LPS involves the activation of $K_v1.5$ and $K_v1.3$ (Pannasch et al., 2006). In $K_v1.5^{-/-}$ mice, the LPS-induced NO production is completely absent, indicating that $K_v1.5$ expression must be necessary for NO production (Pannasch et al., 2006). Just as in myoblasts, $K_v1.5$ could have a key role when predominant (Villalonga et al., 2008). Although $K_v1.3$ may form homotetramers, $K_v1.5$ seems to be mostly involved in heteromers and could be essential for the function of the complex (Pannasch et al., 2006; Villalonga et al., 2007). Similar to what we found in macrophages, DEX inhibits $K_v1.3$ in Jurkat T cells, thereby avoiding Ca^{2+} entry through Ca^{2+} release–activated Ca^{2+} channels (Lampert et al., 2003). Because an increase in Ca^{2+} ions is essential to leukocyte activation (Cahalan and Chandy, 1997), DEX exerts antiinflammatory effects. In addition, down-regulation of $K_v1.3$ impairs T cell volume regulatory mechanisms, which are reversed by transfection with $K_v1.3$ (Lampert et al., 2003). However, this is not the case in macrophages. Cell volume regulatory mechanisms are important during the macrophage immune response. The $K_v1.3/K_v1.5$ composition of the channel assures cell volume control. We found that DEX did not exert changes in the cell size. However, unlike inactivating channels such as $K_v1.4$, $K_v1.5$ is involved in regulatory volume control (Felipe et al., 1993). In this context, DEX up-regulates aquaporins

and amiloride-sensitive osmotic-activated Na$^+$ channels in A549 lung cells and U937 macrophages, respectively; these two types of channels are also involved in the osmotic control (Gamper et al., 2000; Ben et al., 2008).

Unlike LPS, which activates macrophages secreting proinflammatory substances, GCs, used in the treatment of immune-mediated inflammatory diseases, inhibit the expression of many inflammatory mediators. GCs, probably the most powerful endogenous inhibitors of the innate immune reaction across the organism, are mainly synthesized in the adrenal medulla and regulate many cellular functions with both genomic and nongenomic effects. We found that DEX decreased K$_v$1.3 expression without affecting K$_v$1.5. There is a large body of evidence describing discordant DEX effects on channels. Thus, DEX increases K$_v$1.5, but not K$_v$1.4 and K$_v$2.1, expression in pituitary cells in vivo and in vitro (Attardi et al., 1993). In contrast, K$_v$3.2 is rapidly down-regulated in vivo after corticosterone administration in the hippocampus that probably results in enhanced neuroexcitability (Morsink et al., 2007). GCs, also synthesized locally in cardiac cells, induce K$_v$1.5 in the rat heart ventricle and skeletal muscle, but not in the atrium, lung, or hypothalamus (Levitan et al., 1996). We found that DEX did not regulate K$_v$1.5 in macrophages. These results indicate that tissue- and K$_v$ isoform–specific mechanisms may be underlying the corticosteroid endocrine response. For instance, Takimoto and Levitan (1994) found that GCs caused an induction of K$_v$1.5 gene expression in ventricles of adrenalectomized adult rat. K$_v$1.5 contributes to I_{slow} in mouse ventricular myocytes. Contrary to I_{slow}, DEX decreases the density of I_{to} but maintains the biophysical properties and contributes to GC-induced action potential prolongation (Wang et al., 1999). However, differential regulation of K$_v$1.3 and K$_v$1.5 in macrophages leads to molecularly distinct complexes with differentiated biophysical properties. Therefore, changes in the myeloid lineage, mainly due to the heteromeric composition, fine-tune the membrane potential upon immunomodulation.

The relationship between K$_v$ expression and biophysical and pharmacological parameters clearly indicates a trend that fits fairly well with changes in the K$_v$1.3/K$_v$1.5 heterotetrameric ratio. In addition, our findings suggest that in macrophages, this is mostly generated by K$_v$1.3 regulation rather than a change in K$_v$1.5 abundance. Thus, although LPS-induced activation increased the K$_v$1.3/K$_v$1.5 ratio for ~70% of cells, DEX decreased this value in 40% (Fig. 8 A). The biophysical and pharmacological properties were altered in a similar way. The percentage of inhibition, calculated as a function of the remaining fraction in the presence of 750 pM MgTx, the inactivation time constant, and the percentage of cumulative inactivation plotted against the normalized K$_v$1.3/K$_v$1.5 ratio gave Pearson correlation coefficients of r = 0.998, r = 0.965, and r = 0.999, respectively (Fig. 8, B–D).

Although this pattern is similar to what was observed in heterologous expression systems, some differences between models may exist (Vicente et al., 2006). Many heterologous systems do not express the complete machinery to recapitulate the native K$_v$ complex. For instance, HEK-293 cells lack the expression of K$_v$β and KCNE regulatory subunits that are present in native cells (Uebele et al., 1996; Vicente et al., 2005; Arias et al., 2007; Roura-Ferrer et al., 2009; Solé et al., 2009). Diverse K$_v$ channels are produced by tetramerization of channel α subunits that can be encoded by multiple genes. In GH3 pituitary cells, almost all detectable K$_v$1.4 is associated with K$_v$1.5, whereas only ~30% of K$_v$1.5 protein is present as K$_v$1.4/K$_v$1.5 heteromeric channels. DEX specifically increases K$_v$1.5 homomeric channels, but not K$_v$1.4/K$_v$1.5 heteromeric complexes (Takimoto and Levitan, 1996). Thus, hormone induction of one K$^+$ channel subunit gene differentially influences expression of cell surface homomeric and heteromeric channels, leading to specific alteration of excitability. In macrophages, however, pharmacological studies
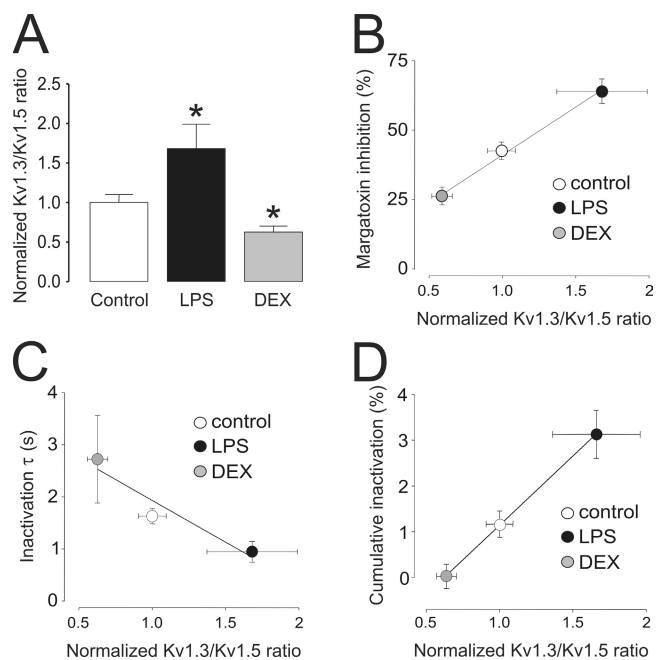

Figure 8. Variations in the K$_v$1.3/K$_v$1.5 ratio correlate with changes in biophysical properties of K$^+$ currents in macrophages. (A) K$_v$1.3/K$_v$1.5 ratios in Raw cells cultured in the presence or absence of LPS and DEX were calculated from real-time PCR experiments in Fig. 4 and standardized to the value of control cells. Values are the mean ± SEM of at least three independent experiments. *, P < 0.05 versus control (Student's t test). (B) Percentage of MgTx inhibition plotted against the K$_v$1.3/K$_v$1.5 ratio. (C) Time constant of inactivation from Fig. 4 (τ) plotted against the K$_v$1.3/K$_v$1.5 ratio. (D) Percentage of cumulative inactivation plotted against the K$_v$1.3/K$_v$1.5 ratio. The Pearson product-moment correlation coefficient using a two-tailed p-value was calculated (P < 0.0393, P < 0.0355, and P < 0.0116 for A, B, and C, respectively). White (bar or circle), control; black (bar or circle), LPS; gray (bar or circle), DEX.

demonstrated that, contrary to pituitary cells, homomeric K$_v$1.5 channels are not present (Vicente et al., 2006, 2008; Villalonga et al., 2007). We therefore assume that K$_v$1.5 form heteromers with K$_v$1.3 in macrophages with properties distinct from homomeric complexes. Similar conclusions have been made in blood-derived dendritic cells in which pharmacological blockade of K$_v$1.3 and K$_v$1.5, and with stable expression of an adenoviral K$_v$1.X dominant negative, suggests a functional role for both proteins (Judge et al., 2006; Mullen et al., 2006). However, by silencing K$_v$1.3, we demonstrated that an increase of K$_v$1.3 subunits, either in homotetrameric or heterotetrameric structures, were mainly responsible for the biophysical changes observed during the LPS-induced activation.

Fig. 9 illustrates several possible heterotetrameric structures in macrophages upon activation and immunosuppression. Macrophages express K$_v$1.3 and K$_v$1.5. Because MgTx abolished K$_v$ currents regardless of the immunomodulatory agent, we can conclude that, similar to human dendritic cells (Zsiros et al., 2009), K$_v$1.5 apparently does not form homomeric complexes. However, the presence of structures solely formed by K$_v$1.3 cannot be ruled out. We have previously shown that, based on biophysical, molecular, and pharmacological studies, the major K$_v$ channel in Raw macrophages is generated by structures where the predominant subunit is K$_v$1.5 (Villalonga et al., 2007). Different K$_v$1.3/K$_v$1.5 ratios are responsible for the biophysical consequences,

fine-tuning the immune response after GC exposure or during an insult.

GCs are secreted in stress conditions. Therefore, they not only affect the cardiac workload, but also the immune response because they are effective repressors of the immune system. Activated GCs are able to interfere with several proinflammatory signaling cascades at different levels. Exogenous GCs are used to treat numerous inflammatory disorders; however, the mechanisms underlying their actions are incompletely understood. Our results could bring some light to this issue because the beneficial effects of GCs in antiinflammatory therapies are linked to K$_v$ channel–mediated immunosuppression. Therefore, the efficacy of GCs in the treatment of inflammatory disorders could be due, at least in part, to their effects on the expression of K$_v$1.3 and K$_v$1.5 channels.
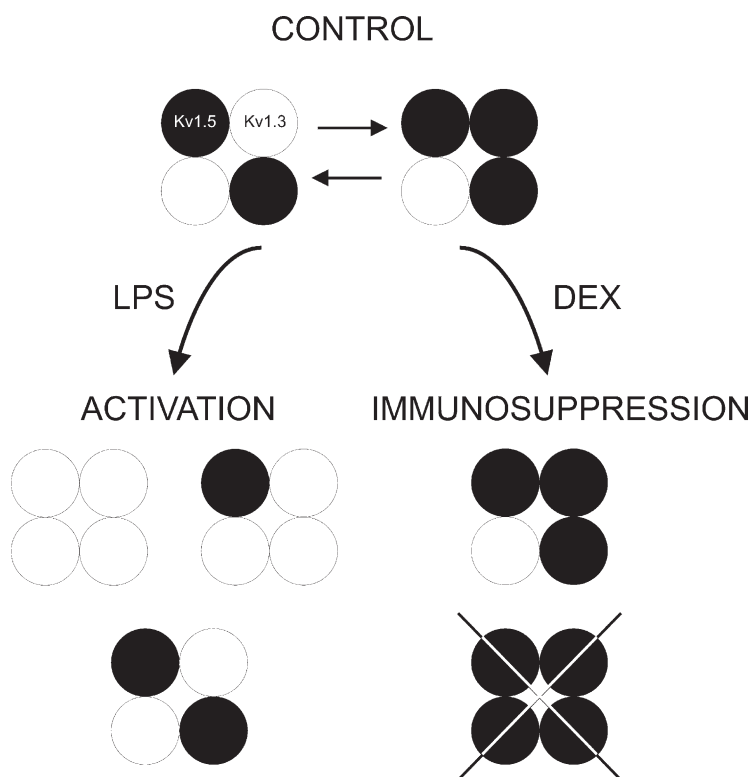
Figure 9. Diagram of major heterotetrameric structures in Raw macrophages upon immunomodulation. Raw cells express K$_v$1.3 and K$_v$1.5. Because MgTx abolished K$_v$ currents, K$_v$1.5 does not form homomeric complexes. However, molecular, pharmacological, and biophysical data indicate that Raw cells express more K$_v$1.5 than K$_v$1.3. LPS-induced macrophages increased the number of K$_v$1.3 subunits at the complex. However, the immunosuppressant DEX decreases K$_v$1.3, which generates K$_v$1.5-predominant heteromeric channels. Different K$_v$1.3/K$_v$1.5 molecular ratios are responsible for the biophysical properties that lead to functional consequences during activation and immunosuppression. White circles, K$_v$1.3; black circles, K$_v$1.5.

REFERENCES

Arias, C., M. Guizy, M. David, S. Marzian, T. González, N. Decher, and C. Valenzuela. 2007. Kvbeta1.3 reduces the degree of stereoselective bupivacaine block of Kv1.5 channels. *Anesthesiology.* 107:641–651. doi:10.1097/01.anes.0000282100.32923.5c

Attardi, B., K. Takimoto, R. Gealy, C. Severns, and E.S. Levitan. 1993. Glucocorticoid induced up-regulation of a pituitary K$^+$ channel mRNA in vitro and in vivo. *Receptors Channels.* 1:287–293.

Ben, Y., J. Chen, R. Zhu, L. Gao, and C. Bai. 2008. Upregulation of AQP3 and AQP5 induced by dexamethasone and ambroxol in A549 cells. *Respir. Physiol. Neurobiol.* 161:111–118. doi:10.1016/j.resp.2007.12.007

Cahalan, M.D., and K.G. Chandy. 1997. Ion channels in the immune system as targets for immunosuppression. *Curr. Opin. Biotechnol.* 8:749–756. doi:10.1016/S0958-1669(97)80130-9

Eder, C. 1998. Ion channels in microglia (brain macrophages). *Am. J. Physiol.* 275:C327–C342.

Felipe, A., D.J. Snyders, K.K. Deal, and M.M. Tamkun. 1993. Influence of cloned voltage-gated K+ channel expression on alanine transport, Rb$^+$ uptake, and cell volume. *Am. J. Physiol.* 265:C1230–C1238.

Fordyce, C.B., R. Jagasia, X. Zhu, and L.C. Schlichter. 2005. Microglia Kv1.3 channels contribute to their ability to kill neurons. *J. Neurosci.* 25:7139–7149. doi:10.1523/JNEUROSCI.1251-05.2005

Franqueza, L., C. Valenzuela, E. Delpón, M. Longobardo, R. Caballero, and J. Tamargo. 1998. Effects of propafenone and 5-hydroxy-propafenone on hKv1.5 channels. *Br. J. Pharmacol.* 125:969–978. doi:10.1038/sj.bjp.0702129

Freedman, B.D., M.A. Price, and C.J. Deutsch. 1992. Evidence for voltage modulation of IL-2 production in mitogen-stimulated human peripheral blood lymphocytes. *J. Immunol.* 149:3784–3794.

Gamper, N., S.M. Huber, K. Badawi, and F. Lang. 2000. Cell volume-sensitive sodium channels upregulated by glucocorticoids in U937 macrophages. *Pflugers Arch.* 441:281–286. doi:10.1007/s004240000410

González, T., M. Longobardo, R. Caballero, E. Delpón, J. Tamargo, and C. Valenzuela. 2001. Effects of bupivacaine and a novel local anesthetic, IQB-9302, on human cardiac K$^+$ channels. *J. Pharmacol. Exp. Ther.* 296:573–583.

Grissmer, S., A.N. Nguyen, J. Aiyar, D.C. Hanson, R.J. Mather, G.A. Gutman, M.J. Karmilowicz, D.D. Auperin, and K.G. Chandy. 1994. Pharmacological characterization of five cloned voltage-gated K$^+$ channels, types Kv1.1, 1.2, 1.3, 1.5, and 3.1, stably expressed in mammalian cell lines. *Mol. Pharmacol.* 45:1227–1234.

Gutman, G.A., K.G. Chandy, S. Grissmer, M. Lazdunski, D. McKinnon, L.A. Pardo, G.A. Robertson, B. Rudy, M.C. Sanguinetti, W. Stühmer, and X. Wang. 2005. International Union of Pharmacology. LIII. Nomenclature and molecular relationships of voltage-gated potassium channels. *Pharmacol. Rev.* 57:473–508. doi:10.1124/pr.57.4.10

Hille, B. 2001. Ion Channels of Excitable Membranes. 3rd ed. Sinauer Associates, Inc., Sunderland, MA. 814 pp.

Judge, S.I., J.M. Lee, C.T. Bever Jr., and P.M. Hoffman. 2006. Voltage-gated potassium channels in multiple sclerosis: overview and new implications for treatment of central nervous system inflammation and degeneration. *J. Rehabil. Res. Dev.* 43:111–122. doi:10.1682/JRRD.2004.09.0116

Kotecha, S.A., and L.C. Schlichter. 1999. A Kv1.5 to Kv1.3 switch in endogenous hippocampal microglia and a role in proliferation. *J. Neurosci.* 19:10680–10693.

Lampert, A., M.M. Müller, S. Berchtold, K.S. Lang, M. Palmada, O. Dobrovinskaya, and F. Lang. 2003. Effect of dexamethasone on voltage-gated K$^+$ channels in Jurkat T-lymphocytes. *Pflugers Arch.* 447:168–174. doi:10.1007/s00424-003-1148-2

Levitan, E.S., K.M. Hershman, T.G. Sherman, and K. Takimoto. 1996. Dexamethasone and stress upregulate Kv1.5 K$^+$ channel gene expression in rat ventricular myocytes. *Neuropharmacology.* 35:1001–1006. doi:10.1016/0028-3908(96)00095-0

Lloberas, J., C. Soler, and A. Celada. 1998. Dexamethasone enhances macrophage colony stimulating factor- and granulocyte macrophage colony stimulating factor-stimulated proliferation of bone marrow-derived macrophages. *Int. Immunol.* 10:593–599. doi:10.1093/intimm/10.5.593

Mackenzie, A.B., H. Chirakkal, and R.A. North. 2003. Kv1.3 potassium channels in human alveolar macrophages. *Am. J. Physiol. Lung Cell. Mol. Physiol.* 285:L862–L868.

Martínez-Mármol, R., N. Villalonga, L. Solé, R. Vicente, M.M. Tamkun, C. Soler, and A. Felipe. 2008. Multiple Kv1.5 targeting to membrane surface microdomains. *J. Cell. Physiol.* 217:667–673. doi:10.1002/jcp.21538

Morsink, M.C., N.G. Van Gemert, P.J. Steenbergen, M. Joëls, E.R. De Kloet, and N.A. Datson. 2007. Rapid glucocorticoid effects on the expression of hippocampal neurotransmission-related genes. *Brain Res.* 1150:14–20. doi:10.1016/j.brainres.2007.02.083

Mullen, K.M., M. Rozycka, H. Rus, L. Hu, C. Cudrici, E. Zafranskaia, M.W. Pennington, D.C. Johns, S.I. Judge, and P.A. Calabresi. 2006. Potassium channels Kv1.3 and Kv1.5 are expressed on blood-derived dendritic cells in the central nervous system. *Ann. Neurol.* 60:118–127. doi:10.1002/ana.20884

Olsson, S., and R. Sundler. 2006. The role of lipid rafts in LPS-induced signaling in a macrophage cell line. *Mol. Immunol.* 43:607–612. doi:10.1016/j.molimm.2005.04.011

Pannasch, U., K. Färber, C. Nolte, M. Blonski, S. Yan Chiu, A. Messing, and H. Kettenmann. 2006. The potassium channels Kv1.5 and Kv1.3 modulate distinct functions of microglia. *Mol. Cell. Neurosci.* 33:401–411. doi:10.1016/j.mcn.2006.08.009

Panyi, G., Z. Sheng, and C. Deutsch. 1995. C-type inactivation of a voltage-gated K$^+$ channel occurs by a cooperative mechanism. *Biophys. J.* 69:896–903. doi:10.1016/S0006-3495(95)79963-5

Panyi, G., Z. Varga, and R. Gáspár. 2004. Ion channels and lymphocyte activation. *Immunol. Lett.* 92:55–66. doi:10.1016/j.imlet.2003.11.020

Park, S.A., Y.C. Lee, T.Z. Ma, J.A. Park, M.K. Han, H.H. Lee, H.G. Kim, and Y.G. Kwak. 2006. hKv1.5 channels play a pivotal role in the functions of human alveolar macrophages. *Biochem. Biophys. Res. Commun.* 346:567–571. doi:10.1016/j.bbrc.2006.05.149

Po, S., D.J. Snyders, R. Baker, M.M. Tamkun, and P.B. Bennett. 1992. Functional expression of an inactivating potassium channel cloned from human heart. *Circ. Res.* 71:732–736.

Pyo, H., S. Chung, I. Jou, B. Gwag, and E.H. Joe. 1997. Expression and function of outward K$^+$ channels induced by lipopolysaccharide in microglia. *Mol. Cells.* 7:610–614.

Roura-Ferrer, M., A. Etxebarria, L. Solé, A. Oliveras, N. Comes, A. Villarroel, and A. Felipe. 2009. Functional implications of KCNE subunit expression for the Kv7.5 (KCNQ5) channel. *Cell. Physiol. Biochem.* 24:325–334. doi:10.1159/000257425

Solé, L., M. Roura-Ferrer, M. Pérez-Verdaguer, A. Oliveras, M. Calvo, J.M. Fernández-Fernández, and A. Felipe. 2009. KCNE4 suppresses Kv1.3 currents by modulating trafficking, surface expression and channel gating. *J. Cell Sci.* 122:3738–3748. doi:10.1242/jcs.056689

Soler, C., R. Valdés, J. Garcia-Manteiga, J. Xaus, M. Comalada, F.J. Casado, M. Modolell, B. Nicholson, C. MacLeod, A. Felipe, et al. 2001. Lipopolysaccharide-induced apoptosis of macrophages determines the up-regulation of concentrative nucleoside transporters Cnt1 and Cnt2 through tumor necrosis factor-alpha-dependent and -independent mechanisms. *J. Biol. Chem.* 276:30043–30049. doi:10.1074/jbc.M101807200

Takimoto, K., and E.S. Levitan. 1994. Glucocorticoid induction of Kv1.5 K$^+$ channel gene expression in ventricle of rat heart. *Circ. Res.* 75:1006–1013.

Takimoto, K., and E.S. Levitan. 1996. Altered K+ channel subunit composition following hormone induction of Kv1.5 gene expression. *Biochemistry*. 35:14149–14156. doi:10.1021/bi961290s

Takimoto, K., A.F. Fomina, R. Gealy, J.S. Trimmer, and E.S. Levitan. 1993. Dexamethasone rapidly induces Kv1.5 K$^+$ channel gene transcription and expression in clonal pituitary cells. *Neuron*. 11:359–369. doi:10.1016/0896-6273(93)90191-S

Uebele, V.N., S.K. England, A. Chaudhary, M.M. Tamkun, and D.J. Snyders. 1996. Functional differences in Kv1.5 currents expressed in mammalian cell lines are due to the presence of endogenous Kv beta 2.1 subunits. *J. Biol. Chem.* 271:2406–2412. doi:10.1074/jbc.271.5.2406

Vicente, R., A. Escalada, M. Coma, G. Fuster, E. Sánchez-Tilló, C. López-Iglesias, C. Soler, C. Solsona, A. Celada, and A. Felipe. 2003. Differential voltage-dependent K$^+$ channel responses during proliferation and activation in macrophages. *J. Biol. Chem.* 278:46307–46320. doi:10.1074/jbc.M304388200

Vicente, R., A. Escalada, C. Soler, M. Grande, A. Celada, M.M. Tamkun, C. Solsona, and A. Felipe. 2005. Pattern of Kv beta subunit expression in macrophages depends upon proliferation and the mode of activation. *J. Immunol.* 174:4736–4744.

Vicente, R., A. Escalada, N. Villalonga, L. Texidó, M. Roura-Ferrer, M. Martín-Satué, C. López-Iglesias, C. Soler, C. Solsona, M.M. Tamkun, and A. Felipe. 2006. Association of Kv1.5 and Kv1.3 contributes to the major voltage-dependent K$^+$ channel in macrophages. *J. Biol. Chem.* 281:37675–37685. doi:10.1074/jbc.M605617200

Vicente, R., N. Villalonga, M. Calvo, A. Escalada, C. Solsona, C. Soler, M.M. Tamkun, and A. Felipe. 2008. Kv1.5 association modifies Kv1.3 traffic and membrane localization. *J. Biol. Chem.* 283:8756–8764. doi:10.1074/jbc.M708223200

Villalonga, N., A. Escalada, R. Vicente, E. Sánchez-Tilló, A. Celada, C. Solsona, and A. Felipe. 2007. Kv1.3/Kv1.5 heteromeric channels compromise pharmacological responses in macrophages. *Biochem. Biophys. Res. Commun.* 352:913–918. doi:10.1016/j.bbrc.2006.11.120

Villalonga, N., R. Martínez-Mármol, M. Roura-Ferrer, M. David, C. Valenzuela, C. Soler, and A. Felipe. 2008. Cell cycle-dependent expression of Kv1.5 is involved in myoblast proliferation. *Biochim. Biophys. Acta*. 1783:728–736. doi:10.1016/j.bbamcr.2008.01.001

Wang, L., Z.P. Feng, and H.J. Duff. 1999. Glucocorticoid regulation of cardiac K+ currents and L-type Ca2+ current in neonatal mice. *Circ. Res.* 85:168–173.

Xaus, J., M. Comalada, A.F. Valledor, M. Cardó, C. Herrero, C. Soler, J. Lloberas, and A. Celada. 2001. Molecular mechanisms involved in macrophage survival, proliferation, activation or apoptosis. *Immunobiology*. 204:543–550. doi:10.1078/0171-2985-00091

Zsiros, E., K. Kis-Toth, P. Hajdu, R. Gaspar, J. Bielanska, A. Felipe, E. Rajnavolgyi, and G. Panyi. 2009. Developmental switch of the expression of ion channels in human dendritic cells. *J. Immunol.* 183:4483–4492. doi:10.4049/jimmunol.0803003